

# Stochastic regularisation of lattice modelling for the failure of quasi-brittle materials

C. Joseph & A.D. Jefferson

*School of Engineering, Cardiff University, Cardiff, United Kingdom.*

**ABSTRACT:** A regular periodic triangular lattice model is developed in this paper to examine the isotropic damage of cementitious materials. The mesh size dependency of current lattice models, which results in a non-unique mechanical response, is addressed through consideration of statistical distributions of lattice beam strengths. The theory of ‘stochastic regularisation’ is presented for a simple 1D parallel bar model, and applied directly to a 2D plane stress lattice discretisation of uniaxial tensile experiments on notched specimens. The main issues to be considered when applying the theory to two dimensions are: (i) stress concentrations at crack tips; (ii) the existence of multiple cracking paths, and; (iii) the increase in ‘effective length’ of beams as damage progresses. These issues are addressed, in part, by the implementation of a two-part strength distribution, which can significantly improve objectivity, whilst maintaining realistic crack patterns without the need for explicit modelling of the mesostructure.

**Keywords:** Lattice modelling, regularisation, fracture mechanics, quasi-brittle materials, concrete.

## 1 INTRODUCTION

Hrennikoff (1941) first introduced lattice models, as a predecessor to finite elements, for solving classical problems of elasticity. Later, Burt & Dougill (1977) extended the method to the simulation of progressive failure of heterogeneous materials. Lattice models have also been used extensively in theoretical physics research at the atomistic scale, and have been used to solve conductivity problems through the application of Kirchoffs laws in fuse networks (Krajcinovic, 1996). Bazant et al.(1990), and Schlangen & van Mier (1992) were the first to extend lattice models to the simulation of progressive failure in concrete using both truss and beam elements.

## 2 LATTICE MODELLING THEORY

The fundamental concept of lattice modelling is that a continuum may be represented by a simple lattice type discretisation of regular or irregular unit cells of resolution length,  $l$ , containing constant or varying coordination numbers (number of ‘half beams’). Generally, the resolution length,  $l$ , is chosen such that it is not too fine to make the analysis unfeasible and not too coarse as to conceal important micro-structural features.

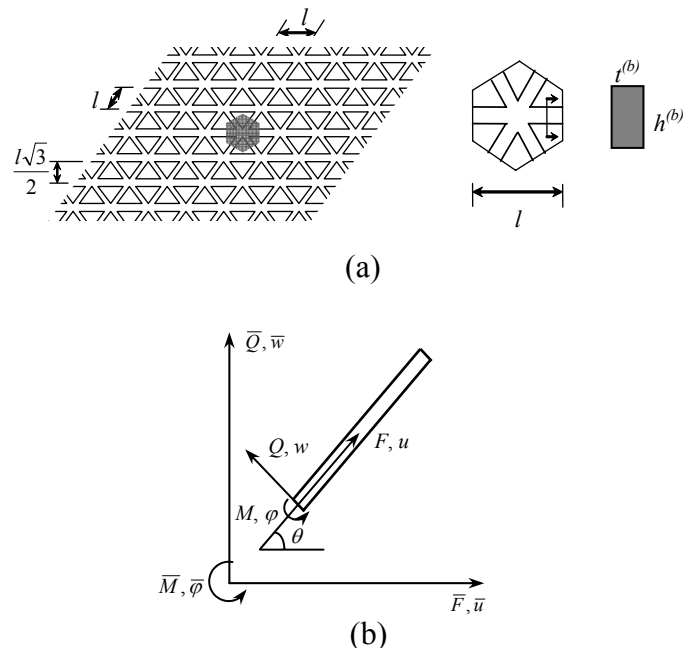


Figure 1. (a) A regular triangular beam lattice with a hexagonal unit cell (b) Element forces and displacements in global and local coordinates.

The lattice considered in this paper is a regular periodic triangular lattice network, with a constant size ( $l$ ) unit cell, and a constant coordination number of 6, as illustrated in figure 1(a). The lattice beam is an Euler-Bernoulli plane frame member, which is

capable of transmitting both moment and shear forces in addition to axial forces, as illustrated in figure 1(b). The structural stiffness of the entire lattice system is obtained from the addition of transformed element stiffnesses according to the topology of the system.

In order for the lattice network to adequately represent the continuum, the properties of the beams must be such that the strain energy stored in a unit cell (figure 1(a)), of volume  $V$ , of a lattice is equivalent to its continuum counterpart under constant strains. A rigorous mathematical description of this equivalence is given by Karihaloo et al. (2003), the main results of which are given in equations 1 and 2;

$$\frac{E}{E^{(b)}} = 2\sqrt{3} \frac{h}{l} \frac{1 + \left(\frac{h}{l}\right)^2}{3 + \left(\frac{h}{l}\right)^2} \frac{t^{(b)}}{t} \quad (1)$$

$$\nu = \frac{1 - \left(\frac{h}{l}\right)^2}{3 + \left(\frac{h}{l}\right)^2} \quad (2)$$

where  $E$ ,  $\mu$ , and  $t$  are the Young's Modulus, Poisson's ratio, and thickness of the continuum, and  $E^{(b)}$ ,  $h$ ,  $l$ , and  $t^{(b)}$  are the Young's Modulus, height, length, and thickness of the beam.

The mesostructure of concrete may be modelled by either (i) implementing a statistical distribution of beam strengths, or (ii) generating a random aggregate distribution, which is overlaid onto a regular triangular lattice to create a three phase model, as shown in figure 2. Beams are assigned equivalent properties of the aggregate, matrix or ITZ (Interfacial transition zone) depending on whether both of their nodes fall within an aggregate particle, within the matrix phase, or on either side of an aggregate-matrix boundary.

A Mohr-Coulomb based failure criterion has been implemented which combines the individual contribution of axial, shear, and centre-span moment in determining the effective stress state of each beam;

$$\mu(\sigma - f_{ib}) + \tau = 0 \quad (3)$$

where  $\sigma$  is the axial stress at the centroid of the beam, including the contribution from the centre span moment,  $\tau$  is the shear stress,  $f_{ib}$  is the rupture strength of the beam, and  $\mu$  is the shear/normal strength ratio.

Re-arranging equation (3) gives the following expression for the effective beam stress:

$$\sigma_{eff} = \sigma + \frac{\tau}{\mu} \quad (4)$$

which is equal to  $f_{ib}$  at beam failure.

### 3 COMPUTATIONAL ASPECTS

The lattice model presented in this paper is a small strain, infinitesimal displacement model. The solution process uses compressed row storage and a Jacobian preconditioned conjugate gradient technique. The pre-processor and main program are written in Fortran 90 and the post-processor is written in Visual Basic 6.

The global stiffness matrix  $\mathbf{K}$  is only formed once, for the case of the pristine, undamaged lattice. Degradation of the system stiffness due to successive removal of fractured beams from the lattice, is achieved by simply removing the broken beams from the global stiffness matrix.

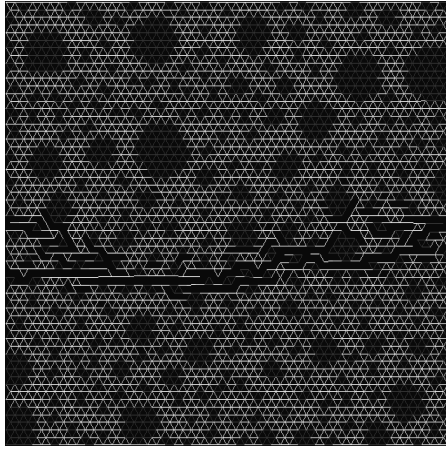
Displacement control is considered in a quasi-static manner; i.e. the displacement is increased until a single beam fails. The new stresses are then calculated and successive removals and re-analyses are performed until stability of the system is achieved, prior to the next displacement increment being applied. The stress state ( $\sigma_{eff} / f_{ib}$ ) of the worst case beam, coupled with the total system displacement, allows the next displacement increment, which will cause this current worst case beam to fail, to be calculated accurately. The ability to automatically fine tune the displacement increment is important, both in ensuring computational efficiency, and maintaining system stability during damage.

### 4 MESH SIZE DEPENDENCY

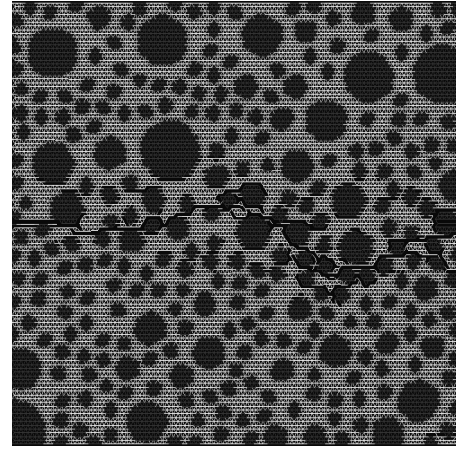
The influence of lattice resolution on the mechanical response of uniaxial tests is highlighted in figure 2, for notched 50mm square concrete specimens. The maximum and minimum aggregate diameters are 8mm and 2mm, respectively, and  $E_{agg} = 87.5\text{GPa}$ ,  $E_{mat} = E_{ITZ} = 31.3\text{GPa}$ ,  $f_{t,agg} = 10\text{MPa}$ ,  $f_{t,mat} = 5\text{MPa}$ ,  $f_{t,ITZ} = 1.5\text{MPa}$ .

It may be seen from figure 2 that both the peak force and the specific fracture energy decrease considerably as the resolution length  $l$  decreases, and hence the non-dimensional lattice size  $\lambda$  increases ( $\lambda = L/l$ , where  $L$  represents the size of the lattice in the direction of uniaxial stress, and  $l$  represents the length of a link). It should also be noted that the mechanical response curve for  $l=0.25\text{mm}$  corresponds well with simulations completed recently by Prado & van Mier (2003) on 60mm square specimens with an aggregate content ( $P_k=51\%$ ) and similar phase properties.

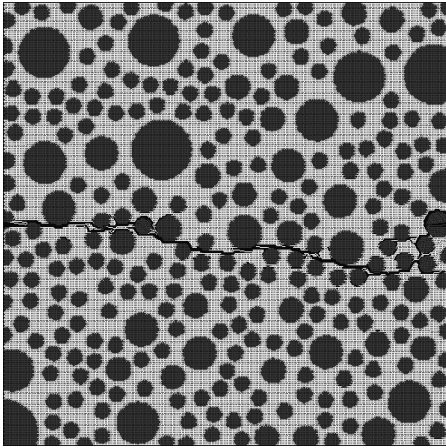
The reason for the observed trend is that the amount of fracture energy per unit area of crack decreases as the size of the lattice beam reduces. Thus,



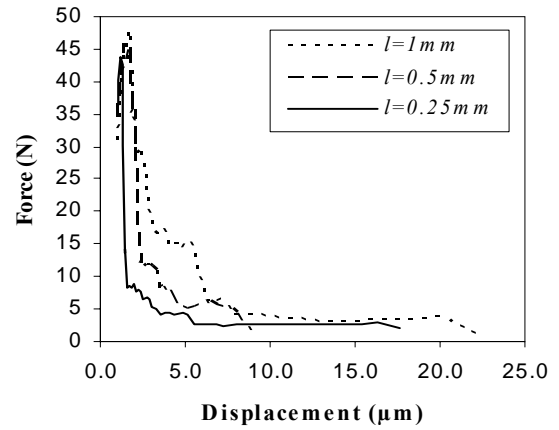
(a)  $l = 1\text{mm}$  ( $\lambda=50$ )



(b)  $l = 0.5\text{mm}$  ( $\lambda=100$ )



(c)  $l = 0.25\text{mm}$  ( $\lambda=200$ )



(d)  $P - \delta$  curves for varying beam lengths

Figure 2. Crack patterns and force displacement curves for 50mm square notched specimens, modelled using varying lattice beam lengths of 1mm, 0.5mm and 0.25mm.

specific fracture energy ( $G_f$ ), or energy release per unit area, is not preserved.

It should be noted that even though the prescribed aggregate content ( $P_k=55\%$ ) is exactly the same for all three simulations in figure 2, the actual ‘modelled’ content varies from 28% for  $l=1\text{mm}$  to 45% for  $l=0.25\text{mm}$ , since the thickness and thus area of the ITZ layer reduces with beam length,  $l$ .

This is not believed to significantly influence the observed mesh size dependence trend, illustrated above, since Schlangen & Garboczi (1997) highlight the same trend for lattices whose heterogeneity is introduced by randomly assigning a ‘high’ strength and ‘low’ strength value to beams in the constant ratio of 3:1.

The lack of uniqueness in the system macro parameters, such as peak strength, and specific fracture energy, is an issue which has been recognised for some time by physicists studying stress driven rupture in central force lattice systems, as discussed by Krajcinovic (1996). Here the size effect has been related to the non-dimensional lattice size  $\lambda$ . Finite scaling laws whereby response curves for lattices of different size  $\lambda$  collapse onto a single master curve plotted in the  $(F\lambda^{-\beta}, u\lambda^{-\gamma})$  coordinate system have also been proposed. The exponents  $\beta$  and  $\gamma$  may then

been determined as fitting parameters from multiple Monte-Carlo type numerical simulations.

It should be noted that this ‘resolution’ length effect is consistent with that found in finite element solutions for fracturing materials, and it is the reason for the introduction of the Bazant & Oh crack band model (1983). Implementing this model within lattice would require the introduction of a tension softening relationship for all beams. Solving for the internal displacements at every load step would then become a non-linear process. Whilst this is possible, and has been implemented for the mortar phase by Karihaloo et al. (2003), the method significantly reduces the computational efficiency of lattice modelling, which is one of its principle benefits, as indicated in section 3.

In addition, regularising in this manner compromises the basic philosophy of lattice, as the authors’ perceive it; namely, that the individual lattice elements should be of such a size that they may be considered to be brittle. It is interesting to note that the systematic rupture of brittle elements during the dissolution of a lattice causes a discontinuous energy release which reflects the ‘energy jumps’ observed during cracking of actual experimental specimens.

This is illustrated by the stepwise form of the softening tail in figure 3(c).

It is also important to note that currently material inhomogeneity is generally modelled solely by the random distribution of aggregate particles prior to superimposition onto the lattice grid. Any stochastic variation of material strength within phases is usually omitted, since all elements of a particular phase are assigned the same properties. van Mier et al. (2002) recently completed an interesting study, however, whereby they assigned both Weibull and Gaussian statistical distributions of properties to lattice beams with the aim of simulating the effects of the mesostructure without explicitly modelling it.

## 5 REGULARISATION THROUGH STATISTICAL SOFTENING

The possibility of including a statistical distribution of beam strengths within the three mesostructure phases, or replacing the mesostructure with a single distribution, which is a function of the lattice resolution length, raises an interesting question; can regularisation be achieved through statistical softening?

### 5.1 1D parallel bar model

Krajcinovic (1996) discusses, in some detail, the application of a Weibull distribution of bar strengths to  $N$  bars in a loose bundle parallel bar model, as illustrated in figure 3(a). Interestingly, the macro mechanical response of such a system under uniaxial tension is similar to that obtained from experimental observations on concrete specimens; i.e. a linear elastic region followed by pre-peak hardening, and post-peak softening. The form of the response curve is governed by the Weibull shape parameter,  $m$ , which is an indication of the material's strength variability; the larger the value of  $m$  the smaller the variability, and the more brittle the response of the parallel bar model.

Alternatively, it is also possible to work from a given softening curve back to a statistical distribution of bar strengths. A standard exponential softening curve, as illustrated in figure 3(b), may be used to represent the stress-strain relationship in the damage zone, which may also be expressed in terms of the damage variable  $\omega$ ;

$$\sigma = (1 - \omega)E\varepsilon = f_t e^{-c_l \frac{\varepsilon_i}{\varepsilon_0}} \quad (5)$$

where  $E$  is the Young's modulus,  $f_t$  is the average tensile strength,  $c_l$  is the softening curve constant,  $\varepsilon_i$  is the inelastic strain, and  $\varepsilon_0$  is the failure strain.

Noting that  $\varepsilon_i = \omega\varepsilon$  and  $\varepsilon_t = f_t/E$ , and approximating the implicit function in terms of the total strain;

$$\omega = 1 - \frac{\varepsilon_t}{\varepsilon} e^{-c_l \frac{\omega\varepsilon}{\varepsilon_0}} = 1 - \frac{\varepsilon_t}{\varepsilon} e^{-c_l \frac{\varepsilon - \varepsilon_t}{\varepsilon_0 - \varepsilon_t}} \quad (6)$$

The aim of the statistical softening model is to replace the softening curve in each bar by a series of bars, which break at different strains, such that the proportion of broken bars in the zone of interest approximates the damage variable  $\omega$ . If there are  $N$  bars and at any point  $i$  bars are broken, and the strain at which a particular bar breaks is denoted by  $\zeta_i$ , and noting that the current total strain on the damage surface is that associated with the strain at which bar  $i$  breaks, then from equation (6);

$$\omega = \frac{i}{N} = \int_{\varepsilon_i}^{\varepsilon_0} p(\zeta) d\zeta = 1 - \frac{\varepsilon_t}{\zeta_i} e^{-c_l \frac{\zeta_i - \varepsilon_t}{\varepsilon_0 - \varepsilon_t}} \quad (7)$$

which is a non-linear equation to be solved for  $\zeta_i$ . A typical response curve for bars whose strengths are distributed according to (7) is shown in figure 3(c). In order for this response to be objective it should be independent of the bar length  $l$ .

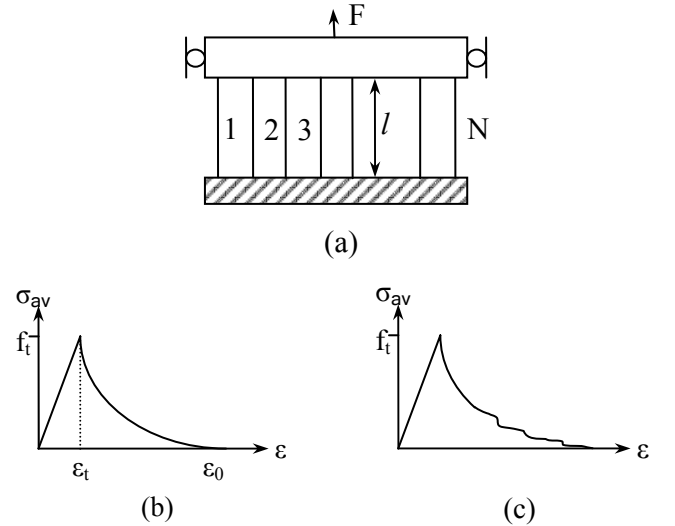


Figure 3. (a) Loose bundle parallel bar model. (b) Target idealised exponential softening curve. (c) Typical macro-mechanical response from discrete parallel bar model.

The key to achieving regularisation is maintaining an average-stress ( $\sigma_{av}$ ) v crack opening displacement ( $u$ ), at localisation, irrespective of the resolution length,  $l$ . If this criterion is to be satisfied, then  $\varepsilon_0$  must be a function of element length, as in the Bazant & Oh (1983) model;

$$\varepsilon_0 = \frac{u_0}{l} \quad (8)$$

where  $l$  is the length of elements in the fracture zone.

Assuming that  $u_0$  is an actual parameter,  $\varepsilon_0$  is therefore inversely proportional to the element length,  $l$ . Thus, by altering the softening curve from which the bar strengths are obtained, and therefore the distribution of these bar strengths, it is possible to maintain a global softening response from the

model irrespective of the element length,  $l$ . This has been confirmed in a 1D parallel bar model by the authors, although the results are omitted here for brevity. It should be noted that the authors have used a simple exponential decay function rather than a Weibull function, since the Weibull function does not allow the softening tail to be scaled whilst keeping the peak the same.

### 5.2 2D lattice model without mesostructure

This theory may be applied directly to a 2D lattice model, as illustrated in figures 4 and 5, for notched 100mm by 50mm specimens. The beam strengths are obtained from equations 7 & 8, for a crack width opening ( $u_0$ ) of 0.2mm,  $f_i = 2\text{MPa}$ , and for resolution lengths of 2mm, 1mm, and 0.5mm. The beam strengths have been distributed randomly throughout the specimen.

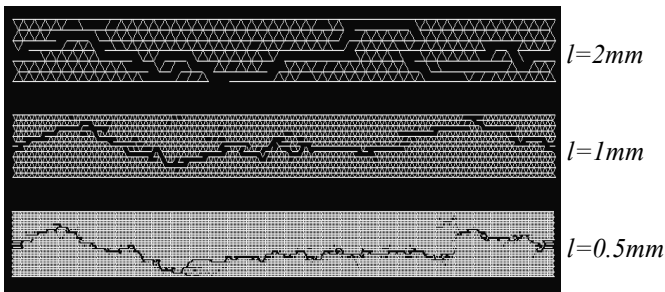


Figure 4. Enlarged crack patterns for 100mm x 50mm notched specimens.

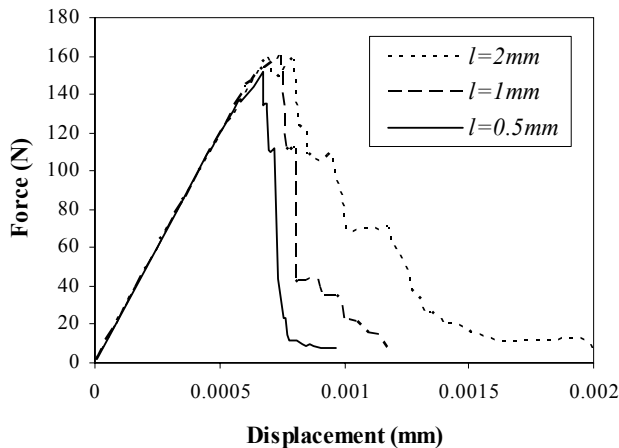


Figure 5. Force displacement graph for 100mm x 50mm notched specimens with varying mesh resolution.

The macro mechanical response of the system (fig. 5) remains unobjective, however, and a trend of diminishing fracture energy with decreasing beam length, similar to that found in figure 2, is still observed.

The reason for this is that the parallel bar model is a mean field artifice, which is incapable of capturing the spatial stress concentrations and redistributions that are prevalent within the 2D lattice model. Adjusting the value of  $\varepsilon_0$  to account for the lattice beam length used in the discretisation (eqn.8), does increase the strength of the strongest beams

significantly, as illustrated in figure 6. This does not, however, significantly influence the mechanical response during failure, since the propagating macro-crack tends to follow the path of 'weakest resistance', rather than localising into a pre-defined single layer of beams. As a result, only the lower portion of relatively low strength beams, as encircled in figure 6, are actually broken. This means that the post-peak response for all three graphs in figure 5 is too brittle, and the final crack mouth opening is approximately 100 to 200 times too small. In addition, since the strength difference between beams of varying length is very small in the lower region of the exponential curves of figure 6, the trend of diminishing fracture energy with element length has not been corrected by any significant degree.

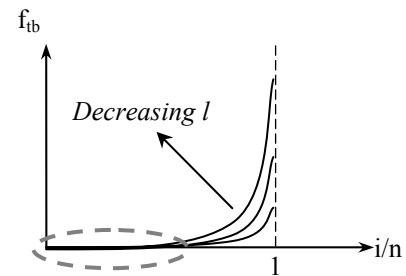


Figure 6. Illustration of beam strength variation with damage for varying lattice beam length.

### 5.3 RME (Representative material element)

In order to adjust the 1D statistical regularization theory for the case of a 2D lattice discretisation, we must first introduce the notion of an RME. An RME is defined here as the smallest region of a lattice discretisation, over which the full array of beam strengths may be found. Since the lattice beam strengths are considered to represent bond strengths within phases of the continuum (weak beams representing ITZ regions and strong beams representing aggregate regions), then the size of an RME is intrinsically linked to the size of an RVE (Representative volume element).

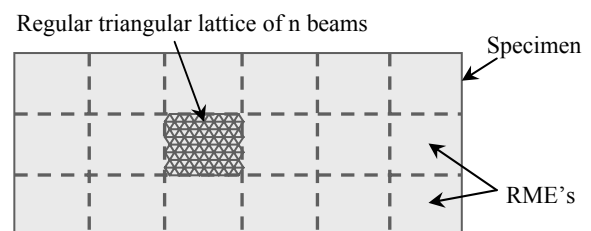


Figure 7. Division of specimen domain into RME's containing n beams.

An RME size, in the order of 3-5 times the maximum aggregate size, as suggested for the case of the crack band model by Bazant & Oh (1983), has therefore been implemented in this model. The total discretised domain has therefore been segregated into RME regions as shown in figure 7, and the full

range of beam strengths have been distributed randomly over each and every RME. It should be noted that since an RME is representative of a materials make-up rather than its constitutive behaviour, as in the case of an RVE, it is considered to exist post-localisation, unlike an RVE (Gitman, 2006).

#### 5.4 Double strength distribution over an RME

The problem of achieving objective results in the 2D lattice may now be considered as the need to regularize the energy release during damage of any given RME.

The number of beams that are fractured during complete failure of an RME is given by;

$$n_\omega = a_\omega n \quad \text{for: } \frac{1.13}{\sqrt{n}} < a_\omega < 1 \quad (9)$$

where  $a_\omega$  is the proportion of total beams that are fractured. The lower limit on  $a_\omega$  is derived from the case when a single horizontal row of diagonal elements break.

If the damage is now considered to be complete (i.e.  $\omega=1$ ) when  $n_\omega$  beams have broken, then;

$$\omega = \frac{j}{n_\omega} = 1 - \frac{\varepsilon_t}{\zeta_j} e^{-c_1 \frac{\zeta_j - \varepsilon_t}{\varepsilon_0 - \varepsilon_t}} \quad \text{for: } 1 \leq j \leq n_\omega \quad (10)$$

where  $\zeta_j$  is the beam strength for beam  $j$ .

However, it is necessary to assign strengths to all beams (1 to  $n$ ) within the RME, in such a way that the distribution for the weakest  $n_\omega$  beams follows equation (10). This is achieved through generating a two-part probability function which matches  $\omega$  in the range 1 to  $n_\omega$  and then increases. It should be noted that since the function given in (10) has almost zero gradient at  $\zeta = \varepsilon_0$  (fig. 8), it is not possible to extrapolate this function to produce a complete distribution for  $n$  beams. The second part of the curve is defined as a Weibull function, where the constant  $m=12$ , noting that the Weibull function form is adopted for convenience only.

$$P(\zeta) = \frac{j}{n} = 1 - \underbrace{\frac{n_\omega}{n} \left( \frac{\varepsilon_t}{\zeta_j} e^{-c_1 \frac{\zeta_j - \varepsilon_t}{\varepsilon_0 - \varepsilon_t}} \right)}_{\text{Part 1}} - \underbrace{\left( \frac{n - n_\omega}{n} \right) e^{-\left( \frac{\zeta_j - \varepsilon_t}{4\varepsilon_0} \right)^m}}_{\text{Part 2}} \quad \text{for: } 1 \leq j \leq n \quad (11)$$

The beam strengths derived from the double strength distribution retain a physical relevance to the underlying mesostructure, despite this not being modelled explicitly. The weaker beams from the first part of the distribution may be considered to represent the ITZ and weaker mortar elements that fracture during propagation of the macro crack. The

stronger beams from the second part of the distribution have little numerical significance, since they should not break, however, physically they may be considered to represent the stronger mortar and aggregate phases.

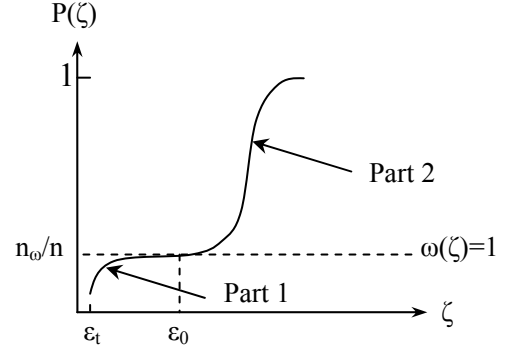


Figure 8. Schematic representation of the two-part probability function.

#### 5.5 Percolation limit

$n_\omega$  is defined as the number of beams that fracture during complete failure of an RME.  $n_\omega$  should be of the order of  $\sqrt{n}$  for a predominantly one dimensional crack propagation in a two dimensional domain. It should be noted that  $n_\omega$  will increase for increasing crack tortuosity and increasing pre-peak damage i.e. distributed beam breakages prior to crack localisation.

Distribution of the  $n_\omega$  beams drawn from the lower part of the double strength distribution is made in a completely random manner within an RME. The proportion of beams which therefore break during complete damage of an RME is therefore considerably less than the proportion of beams that are required to be distributed in order to achieve a percolation path of 'low strength' beams across an RME. For a random distribution of lower strength beams,  $n_\omega$  must therefore be re-defined as;

$$n_\omega = a_p n \quad (12)$$

where  $a_p$  is the percolation limit expressed as a percentage of the total number of beams,  $n$ , in an RME.

Percolation theory in relation to the conductance of lattice networks is discussed at some length by Herrmann & Roux (1990). It should be noted, however, that the stress concentration effects contained within structural lattice networks are omitted in conductance networks. These effects serve to further complicate any theoretical determination of the percolation limit from the mechanical response of the system, since this is dependent on whether the crack path and percolation path coincide.

Also, in contrast to conductance networks, structural lattices, as defined above, do not offer infinite resistance below some percolation limit ( $p_c$ ). Instead, the post peak response becomes increasingly ductile as a result of the need for an increasing proportion of

beams from the upper strength distribution to be broken for complete failure. This may be observed in figure 9, which shows the sensitivity of the post peak softening curve to the percolation limit for a notched 100mm x 50mm specimen with a lattice resolution,  $l = 0.5\text{mm}$ . Conversely, if the proportion of beams drawn from the lower strength distribution is too large, the post peak response becomes overly brittle, since too many percolation paths exist, and thus the stronger beams from the lower strength distribution, which control the softening tail, remain unbroken.

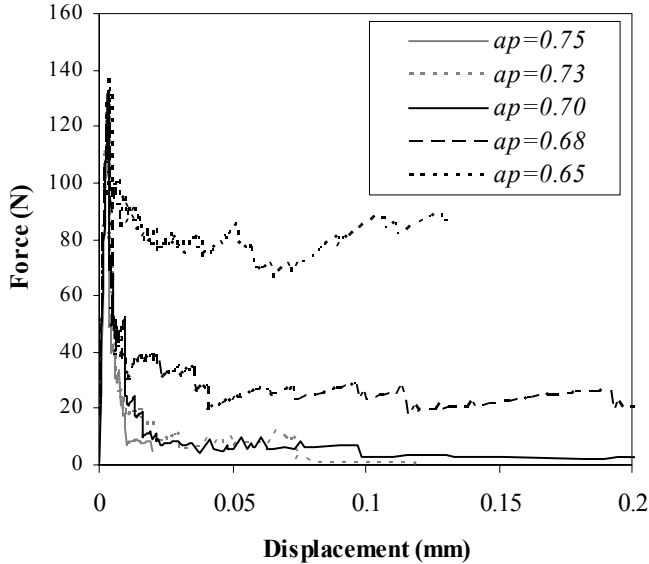


Figure 9. Sensitivity of the post-peak softening response to the percolation threshold  $a_p$ .

From figure 9 it is apparent that an  $a_p$  of 0.7 produces a post peak response which is comparable to the chosen input curve parameters ( $f_i=2\text{MPa}$ ,  $u_0=0.2\text{mm}$ ), and which is representative of a typical cementitious material (van Mier, 1997). It should be noted that a peak load of 140N equates to a peak stress, over the unnotched area, of 1.6MPa. This is less than the peak target stress of 2MPa, due to the initial stress concentrations created by the notches.

The regularisation effect of the double strength distribution method is examined in figure 10 for three different mesh resolutions. Only the length and height of the beams have been altered between lattice resolutions in order to maintain a global Poisson's ratio of 0.2, as given by equation 2.

It may be seen from figure 10 that whilst there appears to be a small decrease in fracture energy in the initial post peak response, the results are largely objective, when allowing for statistical variation. In addition to producing vastly improved quantitative results, the method appears to maintain good qualitative results in respect to predicting feasible crack evolution (fig. 11).

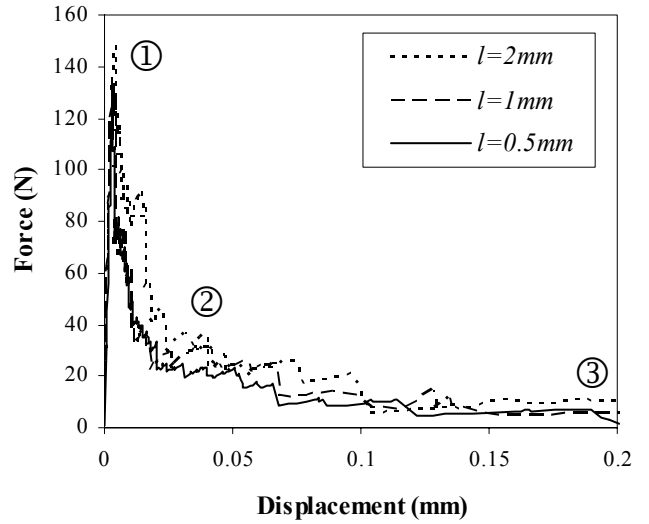


Figure 10. Three typical force displacement graphs for 100mm x 50mm notched specimens with varying mesh resolutions of 2mm, 1mm, and 0.5mm.

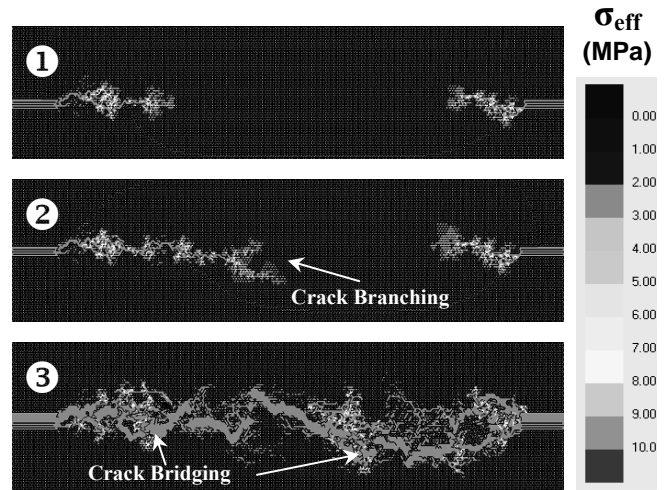


Figure 11. Enlarged views of typical fracture evolution for 100mm x 50mm notched specimen with a 0.5mm mesh resolution (see figure 10 for respective mechanical response).

Figure 11 illustrates the typical evolution of a crack including initial post peak propagation, crack branching, and crack bridging at the end of the softening tail. The amplitude of the crack path is also found to agree well with the chosen size of the RME.

## 6 SUMMARY AND CONCLUSIONS

Lattice models have been recognised for some time as having the ability to disclose important information about the physical processes occurring during the damage of cementitious materials. The quantitative capabilities of the method, in particular, the pathological mesh size dependency, are issues which must be addressed if objective results are to be obtained.

Microstructural disorder is intrinsically linked to the chemical composition, topology and geometry of

the microstructure, as well as micro defects of arbitrary sizes, shapes and orientations. Since the microstructure and defects vary from specimen to specimen, any rational description of the disorder must be fundamentally statistical in nature. Disorder may be modelled within the lattice framework using statistical distributions of beam strengths. It has been shown that in one dimension such distributions may also be modified according to the lattice resolution in order to achieve objective macro parameters such as peak force and specific fracture energy.

Initial results have indicated that the main issues to be considered when applying this theory to two dimensions are: (i) stress concentrations at crack tips; (ii) the existence of multiple cracking paths, and; (iii) the increase in 'effective length' of beams as damage progresses.

These issues have been considered, in part, by the implementation of a two-part strength distribution, which physically represents the materials variability (i.e. weak ITZ bonds, weak-strong mortar bonds, and strong aggregate bonds). The concept of an RME has also been implemented to represent the area over which this entire variability would be expected to be found within the material.

It is believed that by randomly distributing beams drawn from the lower strength distribution, up to the percolation limit, the issues of multiple cracking paths and stress concentrations affecting the choice of crack path, are effectively negated. This means that beams representing the entire lower strength distribution are believed to break during damage. Since the lower strength distribution is responsible for controlling the post peak response, this may therefore be modified in accordance with the chosen lattice resolution to ensure that an average stress - crack opening relationship is maintained.

Initial results obtained from uniaxial tensile tests on 100mm x 50mm notched specimens have indicated that the double strength distribution method vastly improves the objectivity of the macro parameters, such as peak force and specific fracture energy, between varying mesh resolutions. The nature of the post peak response has also been found to be sensitive to the percolation limit. A percolation limit of 0.7 (70% of all beams drawn from the lower strength distribution) has been determined to give an optimal post peak response for a lattice resolution of 0.5mm.

The percolation path created by the random distribution of beam strengths, from the lower strength distribution, across an RME has also been found to give realistic crack patterns without explicit modelling of the mesostructure.

## 7 FUTURE WORK

As with any modelling technique which has an underlying statistical basis, a significant number of

simulations are required in order to draw definite conclusions in regards to the degree of objectivity achieved from the method. Future work will focus on completing these simulations and investigating the effect of lattice resolution on percolation limit.

In addition, it may be observed from figure 11 that during the later stages of damage, large amounts of material are drawn in, thereby releasing disproportionately large amounts of energy on fracture. The nature of the relationship between damage and 'effective' beam length therefore requires investigation.

The model to date has focused on achieving regularisation in respect to eradicating mesh size dependency, however, it may be possible to capture statistical size effects by introducing a statistical distribution of mean RME strengths.

## REFERENCES

- Bazant, Z.P. & Oh, B.H. 1983. Crack band theory for fracture of concrete. *Materials and Structures* 16(93): 155-177.
- Bazant, Z.P., Tabbara, M.R., Kazemi, M.T., & Pijaudier-Cabot, G. 1990. Random particle model for fracture of aggregate or fiber composites. *Journal of Engineering Mechanics* 116(8): 1686-1705.
- Burt, N.J. & Dougill J.W. 1977. Progressive failure in a model heterogeneous medium. *ASCE J Eng Mech Div* 103(3): 365-376.
- Gitman, I.M. 2006. Representative volumes and multi-scale modelling of quasi-brittle materials. Ph. D. thesis, Delft University of Technology, The Netherlands.
- Herrmann, H.J. & Roux, S. (ed.) 1990. *Statistical models for the fracture of disordered media*. Amsterdam: Elsevier / North Holland.
- Hrennikoff, A. 1941. Solution of problems of elasticity by the framework method. *Journal of Applied Mechanics* 12: 169-175.
- Karihaloo, B.L., Shao, P.F., & Xiao, Q.Z. 2003. Lattice modelling of the failure of particle composites. *Engineering Fracture Mechanics* 70(17): 2385-2406.
- Krajcinovic, D. (ed.) 1996. *Damage mechanics*. North-Holland series in Applied Mathematics and Mechanics, ed. J.D. Achenbach, et al. 41. Amsterdam: Elsevier / North Holland.
- Prado, E.P., & van Mier J.G.M. 2003. Effect of particle structure on mode I fracture process in concrete. *Engineering Fracture Mechanics* 70(14): 1793-1807.
- Schlangen, E. & Garboczi E.J. 1997. Fracture simulations of concrete using lattice models: Computational aspects. *Engineering Fracture Mechanics* 57(2-3): 319-332.
- Schlangen, E. & van Mier J.G.M. 1992. Experimental and numerical analysis of micromechanisms of fracture of cement-based composites. *Cement and Concrete Composites* 14(2): 105-118.
- van Mier, J.G.M. (ed.) 1997. *Fracture processes of concrete*. Florida: CRC Press.
- van Mier, J.G.M., van Vliet M.R.A., & Wang T.K. 2002. Fracture mechanisms in particle composites: statistical aspects in lattice type analysis. *Mechanics of Materials* 34(11): 705-724.